كلية الهندسة بشبرا
FACULTY OF ENGINEERING AT SHOUBRA
ERJ
PRINT ISSN 3009-6049
ONLINE ISSN 3009-6022

ENGINEERING RESEARCH JOURNAL (ERJ)
Volume (53),Issue (4)
October 2024, pp:262-270
https://erjsh.journals.ekb.eg

Ergodic Capacity Estimation for 6G Millimeter Wave Smart Metering System in the Presence of Nakagami Fading Channel

Reem Fouad Al-Feky [1,*] ,Adly Tag El_Dien [1] , Sherif Salah [1] , Hesham Mohammad EL-Badawy [2]

[1] Department of Electrical Engineering, Faculty of Engineering at Shoubra, Benha University, Cairo, Egypt.
[2] National telecommunication institute (nti)
**Corresponding author*

E-mail address: reemalfeky2020@gmail.com, adlytag@feng.bu.edu.eg, sherif.salah@feng.bu.edu.eg, hesham@nti.sci.eg

Abstract: Recently, the deployment of 60 GHz technology in smart cities has become one of the main research topics. This paper aims to investigate the connectivity of multiple smart meters within a 60 GHz deployment framework, focusing on Ergodic Capacity (EC) as the primary performance metric. Monte Carlo simulations are employed to analyze the significant influence of spatial distribution on system performance, accounting for factors such as Nakagami-m fading, shadowing, and path loss. To address mm-wave communication blockages, a Poisson Point Process is used to model indoor obstacles, improving simulation accuracy. Mitigation strategies, such as multiple receive antennas and maximum ratio combining (MRC), enhance signal reception and robustness. The analysis shows normalized EC (ε) stabilizes after 100 trials, indicating reliability. Additionally, the paper revealed a trade-off between the number of interfering smart meters (K) and per-meter capacity, with capacity decreasing as more meters connect due to increased interference and reduced bandwidth. The results highlight the superiority of the obtained performance for 802.11ad (WiGig at 60 GHz) with an 11.1% and 20% improvement over the conventional 802.11ac and 802.11ax, respectively. In addition, the presented analysis reveals an asymptotic relationship between the number of interfering smart meters (K) and required SNR, providing valuable insights for planning, deployment, and optimization.

Keywords: Ergodic Capacity (EC), Nakagami fading channel, Smart meters, Smart Grids, Smart city application.

1. Introduction

Smart Cities (SCs) are urban environments that leverage a range of technological tools and sensors to collect data, with the aim of enhancing public resource utilization and service quality, while focusing on comfort, maintenance, sustainability, and reducing operational costs of public utilities. The Internet of Things (IoT), with its potential to utilize sustainable information and communication technologies, is often considered the foundational element of SCs [1-3]. The internet of things, in its broadest sense, refers to the digital interconnection of everyday objects through sensors that gather data from the physical world and transmit it to platforms for processing into actionable information. In the context of SCs, the data transmitted to the server via the gateway and detected by sensors or actuators forms the core structure of the IoT [4]. With the proliferation of smart devices, there is a growing interest in connecting and integrating various items through existing networks. These smart devices aim to share and access information with other devices, enabling them to make intelligent decisions. The objective is to integrate these devices seamlessly into existing infrastructure, thereby maximizing their compatibility and interoperability. One such complex technology is the Smart Grid (SG) system, which can provide accurate information and power, delivering them efficiently. It also possesses several other features, including accessibility, accuracy, flexibility, interoperability, maintainability, measurability, dependability, sustainability, and stability [5]. The two-way communication in smart grids, acting as a conduit between the data collection terminal and the processing terminal, is a key differentiator between smart grids and traditional grids. This opens up numerous advantages, including the use of distributed smart sensors, distributed power generation, real-time measurements and metering infrastructure, monitoring systems, and reliable communication for information exchange [6]. To manage such a complex system, a robust architecture with continuous device inspection and monitoring is necessary. This requirement can be fulfilled by the Smart Metering System (SMS), which consists of smart meters and communication infrastructures. The advent of the 5G era brings new network and service capabilities, such as massive bandwidth, low power consumption, and low latency, which can enable additional smart city application scenarios for mobile networks. Moreover, 5G will be a critical component of a true IoT, facilitating a new type of communication network that connects everyone and everything. This platform will allow for the connection of a vast array of sensors and actuators with stringent energy efficiency and transmission requirements [7,8]. The utilization of millimeter waves (mm-Waves) within the frequency range of 60 GHz to 300 GHz is a proposed modification. This frequency band's substantial capacity makes it ideal for fifth-generation (5G) and future cellular networks. Owing to its broad spectrum, resistance to interference, and ability to create a conducive environment for monitoring and control tasks, the transmission in the mm-Wave band is quickly becoming the preferred choice for Smart Grids (SG) [9]. Notable characteristics of millimeter waves include significant penetration loss, which hinders their passage through construction materials like walls, and susceptibility to air attenuation and absorption caused by rain and humidity [10]. Therefore, in the context of future cellular networks, millimeter-wave (mm-Wave) communication has emerged as a promising candidate to meet the capacity demand in densely populated indoor environments. Related works represent the performance of mm-Wave communication systems, including coverage probability [11-12]. Due to the flexibility of stochastic geometry in mathematics, it has been used to examine mm-Wave networks in a variety of ways, including the analysis of coverage performance in cellular mm-Wave networks [13–15]. In [16], researchers have investigated a millimeter-wave Multiple-Input, Multiple-Output (MIMO) system incorporating Maximal Ratio Combining (MRC). The focus of the study was to determine the probability density function of the array output Signal-to-Noise Ratio (SNR) in this MIMO-MRC setup. A mathematical formula that directly calculates the outage probability of a device-to-device (D2D) user in mm-Wave integrated D2D communication systems under Nakagami-m fading channels was presented. This formula accounts for scenarios where multiple cellular or D2D users create interference during mm-Wave integrated D2D transmission [17]. The stochastic geometry techniques were employed to evaluate the uplink performance of millimeter-wave (mm-Wave) cellular networks with device-to-device (D2D) capabilities. The analysis focused on determining the signal-to-interference-plus-noise ratio (SINR) outage probability for both the cellular connections and D2D links [18]. Furthermore, a manageable uplink modeling framework has been developed to bolster the multi-tier millimeter wave (mm-Wave) cellular networks' signal-to-interference-and-noise-ratio (SINR) outage probability [19]. This framework considers the probability of Line-of-Sight (LoS) and various channel fading's for LoS and Non-Line-of-Sight (NLoS) links, thereby examining the impact of interference on Unmanned Arial vehicle (UAV) communications. Subsequently, a closed-form outage probability was derived for all potential environments of primary and interference connections in the presence of an interfering node [20]. The performance of six transmission methods was assessed by developing throughput and outage probability, utilizing the Nakagami-m fading channel to investigate the effects of propagation channel conditions, for both of LoS and NLoS operational scenarios [21].

Recent papers have further extended analysis for the ergodic capacity estimation for mm-Wave systems, particularly in the context of Smart Cities and 5G/6G networks. Dilli [22], conducted a performance analysis of multi-user massive MIMO hybrid beamforming systems at mm-Wave frequency ranges. The study highlighted the potential of hybrid beamforming in improving the ergodic capacity of mm-Wave systems, which is crucial for high-speed data transmission in Smart City environments. Zhang and Liu [23], provided an ergodic capacity analysis on MIMO communications in the Internet of Vehicles (IoV). Their work underscored the importance of MIMO technology in enhancing the capacity of vehicular networks, a key component of smart transportation systems. Another study by Zhang and Liu [24], further emphasized the significance of ergodic capacity analysis in IoV communications, reinforcing the need for robust communication systems in dynamic urban settings. Omer et al [25], presented an evaluation of mobile system performance based on ergodic capacity, offering insights into the performance of mobile networks in Smart City applications. Hassan and Moinuddin [26], explored beamforming techniques using exact evaluation of leakage and ergodic capacity in multi-user MIMO systems. Their findings demonstrated the potential of advanced beamforming techniques in optimizing the capacity of wireless networks. Salimian Rizi and Falahati [27], conducted an analysis of ergodic capacity and symbol error rate in a wireless system with α-μ composite fading channels. This study was particularly relevant to Smart City environments, where diverse fading conditions could significantly impact communication performance.

The main contribution of this the presented work aims to determine the trade-off between the number of smart meters and the achieved normalized Ergodic Capacity (EC) (which will be denoted by ε) at different signal-to-noise ratios (SNR). This analysis enables system designers to make informed decisions about the number of smart meters to be deployed. They can use this information, along with estimated SNR levels in the Smart City environments, to meet target performance requirements. Furthermore, our work investigates the impact of random smart meter (SM) placement compared to equally spaced deployments, offering insights relevant to real-world deployment scenarios. Employing Monte Carlo simulations in the presence of blockages (obstacles) (modeled using a Poisson Point Process) and without blockages. So, the presented work evaluates system performance using the Ergodic Capacity (EC) as the main key performance index (KPI), assuming Nakagami-m fading characteristics for the communication channel. In addition, this paper provides valuable insights for selecting a smart metering system localization method, clarifying the advantages and disadvantages of equally spaced versus random localizations. In addition, it highlights the significant influence of blockages and interference from neighboring smart meters on the overall system performance.

The remaining sections of the paper are organized as follows: Section 2 presents the system model; Section 3 focuses on deriving the analytical performance based on EC metric. Section 4 presents the analytical and simulation results, and finally, Section 5 provides our conclusions based on the findings.

2. SYSTEM MODEL

Figure 1 illustrates our proposed indoor smart metering system model. The system comprises K+1 smart meters, each equipped with a single transceiver antenna. Smart Meter 0 (SM0) serves as the main reference node, while the remaining K smart meters act as potential interferers. All smart meters communicate with a central gateway, which is equipped with N_r receive antennas. The gateway employs Maximum Ratio Combining (MRC) to enhance signal reception and improve link reliability. This technique allows the gateway to optimally combine signals received across its multiple antennas, effectively mitigating fading and interference effects.

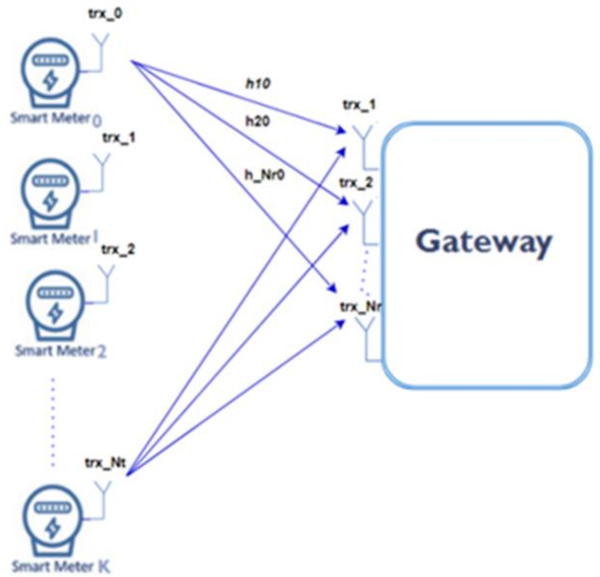

Figure 1. Block diagram of SMS.

Due to significant penetration losses of millimeter waves (mm-Waves) through construction materials, interference from SMs in neighboring buildings is negligible. This effectively isolates indoor networks within each building. For reliable communication over the millimeter wave channel, accurate wireless channel models are essential. These models may differ from those used for standard radio frequency (RF) channels. As shown in [28,29], performance parameters including coverage probability, outage probability, ergodic capacity and error probability may be analyzed using statistical models of the channel. It has been demonstrated that the Nakagami-m distribution is capable of simulating the statistics of small-scale fading for a number of channels, including the millimeter-wave channel [30]. At each receiving antenna, the signal is subjected to Additive White Gaussian Noise (AWGN) with zero mean and variance σ^2 , which is expressed by $n(t)$.

At a specific moment t, the i_{th} node transmits the signal $S_i(t)$, assuming that the transmitted power of SM_i is represented by P_i. The vector $r(t)$ refers to received signals received at N_r antennas [31].

$$r(t) = \sum_{i=0}^{K} h_i S_i(t) + n(t) \tag{1}$$

Where h_i is the channel gain vector of the i_{th} smart meter, and K is the total number of smart meters.

Then the output signal $y(t)$ after applying MRC technique with weight vector W=h_0 , will be

$$(t) = h_0^H h_0 S_0(t) + \sum_{i=1}^{K} h_0^H h_i S_i(t) + h_0^H n(t) \tag{2}$$

Where H denotes **Hermitian matrix**.

2.1 Blockage Model

The potential sources of blockage for mm Wave in indoor environments include humans, furniture, and concrete structures. In this section, we describe the blockage model. As mentioned in [32], there are many models that can comprehensively estimate the real-time blockage loss of signals using mathematical schemes. In this section, the indoor environment is represented by an enclosed space denoted as A, with dimensions L (length) × W (width) × H_c (height of ceiling) as illustrated in Fig. 2.

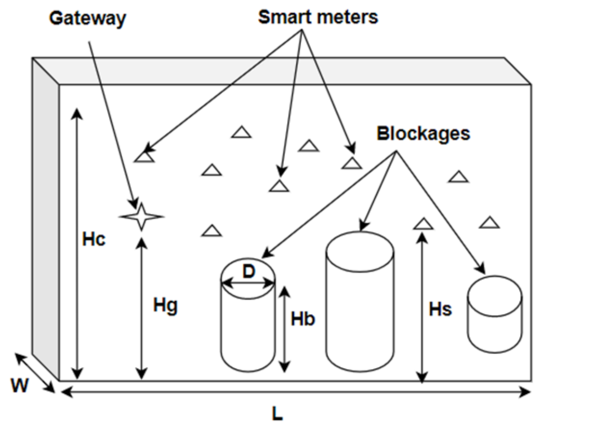

Figure 2. Blockage model.

Not all blockages in the environment affect the actual propagation path between the gateway and the smart meter. As illustrated in Fig.3, there are two types of blockages: a) Blockages that do not intersect the propagation path, b) Blockages that intersect the horizontal axis at a point r, where r is the distance between the blockage and the gateway. A blockage of type (b) potentially blocks the path if its height is larger than the effective height H_{eff} at that distance.

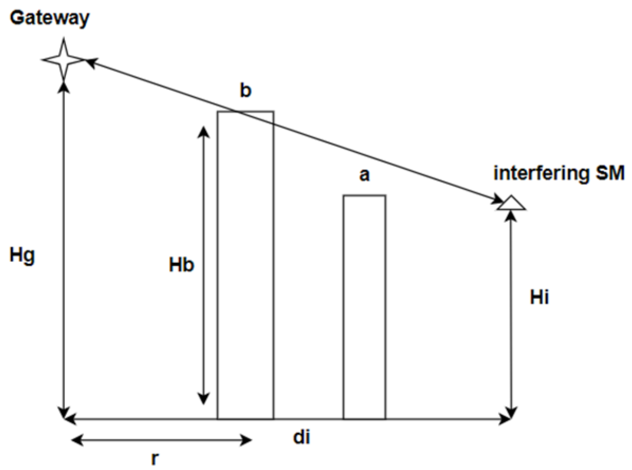

Figure 3. Blocking scenario

The blockages within the space are randomly distributed using Poisson Point Process and modeled as cylinders with intensity I. These cylinders represent the physical dimensions of the blockages, with random height H and diameter D which are uniformly distributed between $h_{min}, h_{max}, and\ D_{min}, D_{max}$

respectively. The random distribution implies that the blockages can be located anywhere within the enclosed space A, without any specific pattern or arrangement. We assume that all SMs have the same height H_s above the ground, and the gateway located at the height H_g , as H_s and H_g ∈[0, H_c]. The effective height H_{eff} is calculated using the following formula [31]:

$$H_{eff} = \left(\frac{H_g - H_s}{d_i}\right) * r + H_s \tag{3}$$

Where d_i is the distance between each interfering SM and gateway.

Since the blockage's height exceeds the effective height of the obstacle at that distance, it effectively blocks the propagation path, causing a significant reduction in signal strength or complete interruption of the signal along that path.

2.2 Path Loss Model

Path loss is a significant factor influencing the performance of mm-wave communication and holds crucial importance in the design of efficient and reliable systems capable of achieving high data rates. Signal attenuation occurs when the transmitted signal travels through the communication channel and is affected by factors such as distance and the characteristics of the propagation channel in both LoS and NLoS operational scenarios. This phenomenon results in a decrease in signal strength during propagation. Path loss stems from multiple factors, such as natural radio wave expansion, diffraction caused by obstructions, and absorption due to media that restrict the transparency of electromagnetic waves. Diffraction is the phenomenon of waves bending around obstacles or apertures. Diffraction losses occur when an obstacle partially or completely blocks the LoS path between the transmitter and receiver. Diffraction losses depend on the size and shape of the obstacle, the wavelength of the signal, and the angle of incidence. According to IEEE 802.11ad, which is a standard for wireless communication at 60 GHz frequency, diffraction losses are negligible for most indoor scenarios. This is because the wavelength of the signal at 60 GHz is very small (about 5 mm), and the typical obstacles in indoor environments are large compared to it. Therefore, the signal cannot bend around the corners of the obstacles and create sharp shadow zones behind them [33,34]. Moreover, IEEE 802.11ad uses directional antennas and beamforming techniques to focus the signal energy in a narrow beam, which reduces the chances of encountering diffraction obstacles. Consequently, most of the transmission power is propagated between the transmitter and receiver through line-of-sight and low-order reflection paths, resulting in a quasi-optical propagation channel [35]. Various path loss models have been proposed and investigated for indoor mm-wave channels, particularly in the mm-wave frequency bands [36, 37]. The Close-In (CI) Free Space Path Loss Model is a widely used model that is primarily based on the anchor point and the frequency in the free space [36]. This model depends on the carrier frequency of the propagating signal (f in GHz), the three dimensional distance between the transmitter and the receiver (d in meters), and the selected reference distance ($d_{ref} = 1m$). Equation for the model is

$$PL^{CI}(d)[dB] = FSPL\big(f, d_{ref}\big)[dB] + 10.n.log\left(\frac{d}{d_{ref}}\right) + X_\sigma^{CI} \tag{4}$$

Where:

$PL^{CI}(d)$ is the path loss in dB at distance d using the CI model, $FSPL\big(f, d_{ref}\big)$ is the free space path loss in dB at the reference distance d_{ref} for frequency , f is the carrier frequency in GHz, n is the path loss exponent, characterizing the rate of signal attenuation with distance in the given environment, X_σ^{CI} is a zero-mean Gaussian random variable with standard deviation σ in dB, representing the shadowing effect.

3. PERFORMANCE METRIC

Ergodic Capacity (EC) represents the expectation of the maximum achievable rate over a set of environmental channels. It considers adaptive transmission strategies and accounts for varying channel states, providing insights into wireless communication system performance.

$$EC = E\{log_2(1 + \gamma)\} \tag{5}$$

Where E[•] is the expectation operator, defined by averaging the Shannon capacity over the probability density function (PDF) of the overall instantaneous SINR (γ) that could be calculated as follow [31].

$$\gamma_{MRC} = \frac{P_0|h_0|^2}{\sum_{i=1}^{K} P_i|h_i|^2 + \sigma^2} = \frac{\rho_0\,|h_0|^2}{\sum_{i=1}^{K} \rho_i|h_i|^2 + 1} \tag{6}$$

Where $\rho_0 = \frac{P_0}{\sigma^2}$ is the transmit SNR of main SM, and ρ_i for i={1,…,K}. represents the transmit SNR at each interfering SM.

Our channel model contains a Nakagami fading component, path loss as well as shadowing. Nakagami-m wireless channel with fading and spread parameters m_l and Ω_l for LoS and m_N and Ω_N for NLoS, respectively, is represented as $|h_i|^2$, 0 ≤ i ≤ K. Given that the Nakagami-m distribution that characterizes the wireless channel, $|h_i|^2$ will have a Gamma distribution whose PDF and CDF are as follows [38]:

$$f_{|h|^2}(x) = \left(\frac{m_l}{\Omega_l}\right)^{m_l} \frac{x^{m_l-1}}{\Gamma(m_l)}\, e^{-\left(\frac{m_l}{\Omega_l}\right)x} \tag{7}$$

$$F_{|h|^2}(x) = 1 - e^{-\left(\frac{m_l}{\Omega_l}\right)x} \sum_{m=0}^{m_l-1} \frac{\left(\left({m_l}/{\Omega_l}\right)x\right)^m}{m!} \tag{8}$$

Where $\Gamma(m) = \int_0^\infty t^{m-1}e^{-t}\,dt$ is the Gamma function.

4. RESULTS & ANALYSIS

In this section, we employ Monte Carlo simulations in order to study the performance of our model in different scenarios, both with and without blockages, respectively. In the following results, we will investigate several topics, which can be summarized as follows: required number of simulation trials in order to achieve the convergence of the obtained normalized EC (ε). In addition, we will try to obtain an asymptotic relationship between the number of smart meters and the achievable normalized EC (ε) at specific SNR levels. The system parameters used are illustrated in Table 1.

TABLE 1. System Parameters [31]

System parameter	symbol	value
Number of interfering SMs	K	43
Distance between the gateway and the Main SM	d_o	5m
Distance between interfering SMs	d_i ; $1 \leq i \leq K$	2m < d < 50m
Nakagami fading parameter for LOS link	m_L	4
Nakagami fading parameter for NLOS link	m_N	2
Nakagami spread parameters for LOS &NLOS links	$\Omega_L = \Omega_N$	1
Path-loss exponent for LOS link	α_L	2
Path-loss exponent for NLOS link	α_N	4
Intensity of blockages	I	0.3 blockages/m^2
The mean of shadowing factor	μ	0
The standard deviation of shadowing factor	σ	10
Diameter of blockages	D	0.2m < D < 0.8m
Height of blockages	H_b	0.1m < H_b <1.7m
Height of smart meters	H_s	1.3m
Height of Gateway	H_g	4m
Length of enclosed area	L	50m
width of enclosed area	W	50m

In order to investigate the effect of the localization criteria for the Smart Meters under study, we are proposing the distribution of its localization as in Fig.4. Figure (4) illustrates the distribution of a random localization for 43 interfering smart meters (K=43). The selection of the number of SMs is in consistence with [31], but we are assuming more generic deployment scenario by permitting of the random placement for each SM. Whereas, in [31], authors were assuming optimistic system deployment by having equally space SMs. The deployment area is taken 50m x 50m. The other system parameters are taken based on the system model that had been studied in [31]. The "Main SM" is positioned at d_o = 5 meters from the gateway, serving as a reference point for performance analysis of other SMs in similar conditions. Each interfering SM's distance to the gateway is represented by d_i. This indoor deployment scenario is characterized by the proximity of SMs to the gateway, ensuring effective communication within a limited space.

Figure (5) presents a comparative analysis of normalized EC (ϵ) between the proposed model and the model that was discussed in [31], considering scenarios both with and without blockages. In [31], the authors assumed a homogenous distribution of interfering smart meters, with equal inter-separation distances for K=43, d_o=5m, and ρ_i=20dB, i={1,…,K}.

It is evident from Figure 5 that the normalized EC (ε) of both models reach to convergence as the number of trials increases. After approximately 100 iterations, the system achieves sustainable performance parameters. This suggests that beyond this point, more stable system performance will be achieved. Therefore, during the course of this study, we will perform 200 iterations to ensure that the system performance metrics fall within the convergence range.

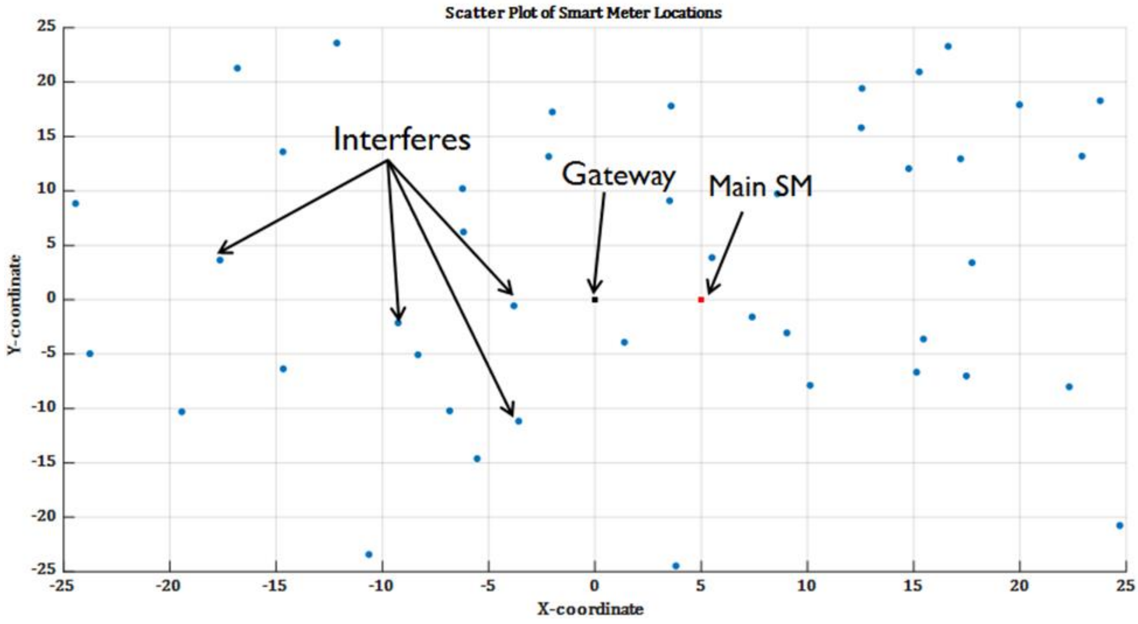

Figure 4. Main components of SMS.

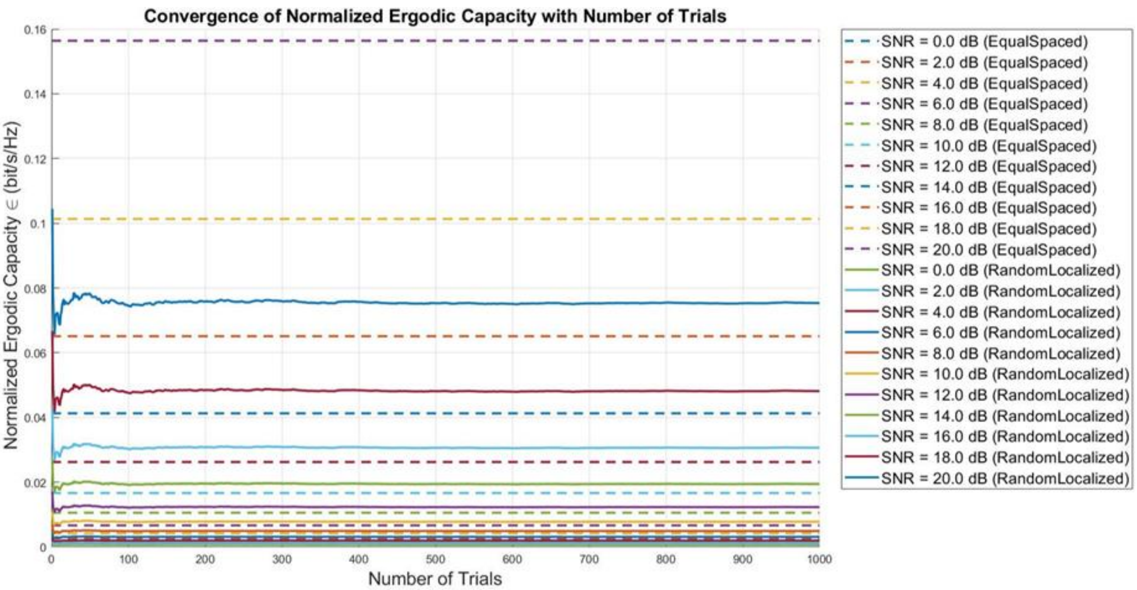

(a) Without blockages

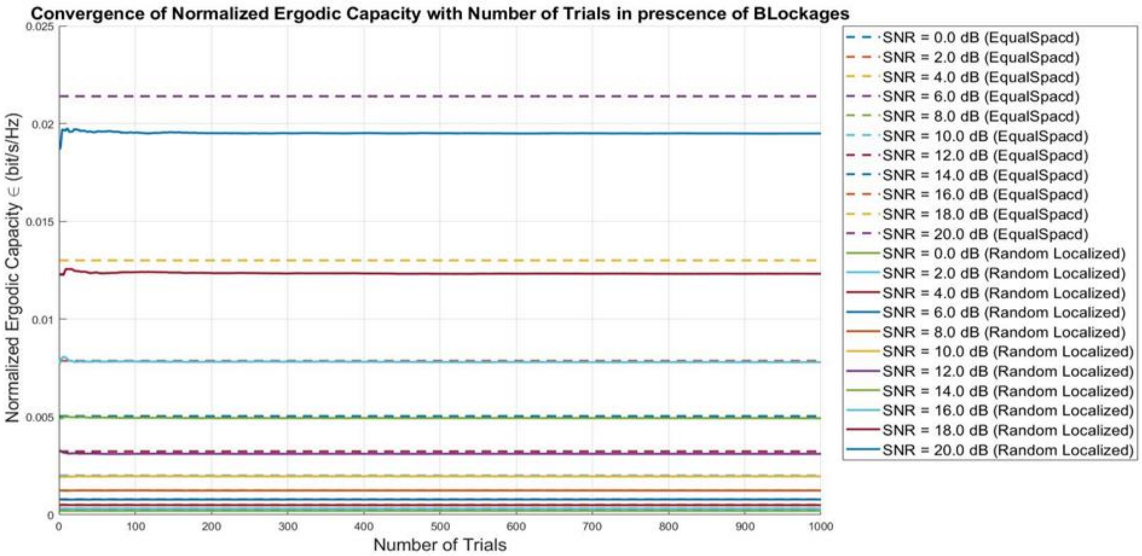

(b) With blockages

Figure 5. Normalized Ergodic Capacity (ε) vs. number of trials for different SNR levels in following cases: **(a)** without blockages and **(b)** with blockages.

Additionally, in Figures 5(a) and 5(b), we notice that the equally spaced model operates at a higher capacity compared to the randomly localized model. This is due to the more stable and homogenous operational channel conditions, which cannot be found in real life deployment scenarios. Consequently, the overall system capacity is degraded in the presence of non-homogenous interfering conditions. In contrast, our concurrent model reflects a more realistic scenario, assuming different separation distances between smart meters, exhibiting more variability.

Figure (6) illustrates the relationship between normalized EC (ε), Number of interfering Smart Meters (K) for different SNR levels focusing on how normalized EC (ε) of a single meter (main SM) change with number of interfering devices.

Figure (6) shows that capacity decreased by increasing the number of connecting smart meters. On the other hand, by increasing number coexisting meters in same bandwidth, the co-channel interference will be enlarged. So that, the obtained system performance parameters will be degraded not only due to sharing same system radio resources but also, due to co-channel interference that could be caused by more and more engaged meters. In addition, Fig.6 shows that the higher SNR levels consistently result in higher capacity, regardless of the number of smart meters. This emphasizes the importance of strong signal strength in maintaining optimal network performance, especially as smart meters density increases. To summarize the obtained system parameters, Table 2 provides a comparison of different wireless technologies.

It highlights the recommended technology mentioned in [39] and allows for a detailed analysis of the results for each system.

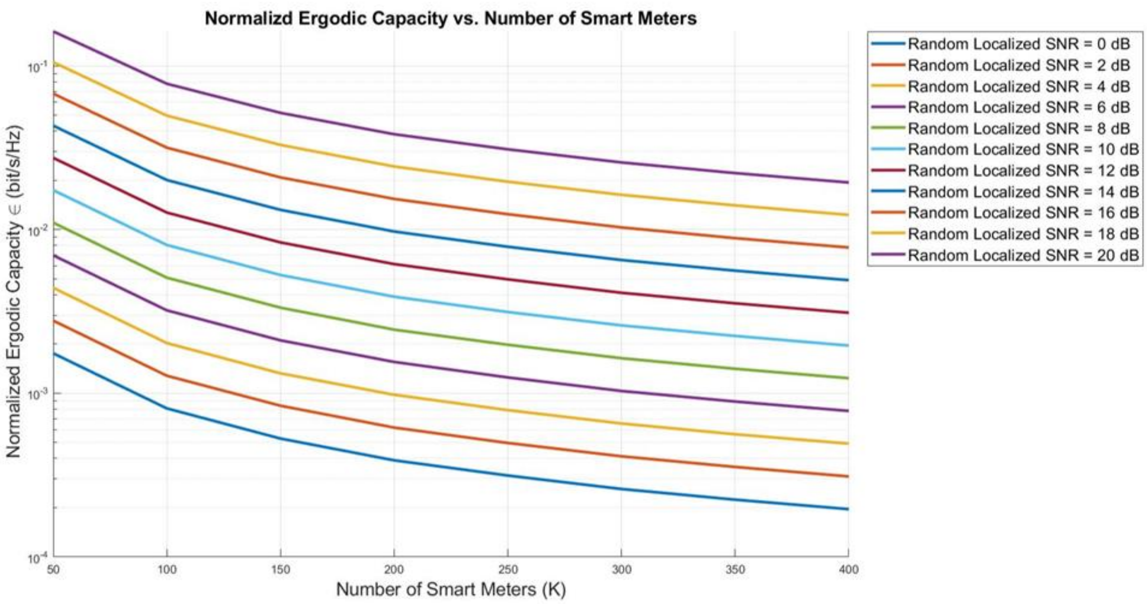

Figure 6. Normalized Ergodic Capacity (ε) vs. number of SMS (K) for different SNR levels.

TABLE 2. Comparison between different wireless technologies

Wireless Technology	Channel Bandwidth	Maximum Data Rate	Spectral Efficiency bps/Hz	Max (ϵ), bps/Hz Per meter K=400
Zigbee	2 MHz	~250 kbps	0.125	0.0003125
Wi-Fi 802.11ac	40MHZ	~200 Mbps	5	0.0125
Wi-Fi 802.11ax	40MHZ	~287 Mbps	7.2	0.018
Wi-Fi 802.11ad	2.16 GHz	~7 Gbps	3.2	0.008

Table 2 highlights performance normalized EC (ε) threshold for each technology, these results will be used to investigate the potential advantages of higher bandwidth technologies for future smart grid applications. Wi-Fi 802.11ad, operating in the 60 GHz band (considered extremely high frequency, EHF), illustrates significantly higher data rates compared to Zigbee. This capacity for increased data transfer makes technologies looks like 802.11ad is a suitable candidate for supporting the expansion of smart grid functionalities, such as real-time energy monitoring and demand-side management, which cannot be supported by existing Zigbee-based systems.

Figure (7) investigates the relationship between Signal-to-Noise Ratio (SNR) and the number of interfering smart meters (K) supported for various wireless technologies commonly deployed in smart meter, by leveraging the normalized EC (ε) values, as outlined in last column in table 2, and extrapolating them onto a scenario analogous to Fig.6. Figure (7), reveals that capability of 802.11ad (WiGig at 60GHz) to provide higher performance in terms of supporting a larger number of devices as the Signal-to-Noise Ratio (SNR) increases. This is reflected by the steep increase in the number of served meters (K) (marked with red on figure (7)). Notably, 802.11ad can support approximately 400 devices at an SNR around 16 dB, whereas the other competitive technologies such as 802.11ac and 802.11ax require higher SNR levels to achieve similar performance. This indicates that 802.11ad can maintain high performance even at lower SNR levels, which is advantageous for scenarios with constrained signal quality. Furthermore, the relationship between the number of interfering smart meters (K) and SNR can be mathematically approximated using the following asymptotic relation:

$$K = a.e^{(b.SNR)} \tag{10}$$

Where a, b are constants that would need to be adjusted for each specific technology to achieve the best fit as shown in Table 3. This extrapolated formula provides a supportive guide for estimating the capacity of different wireless technologies under varying SNR conditions in smart meter deployment scenarios.

Table 3. Constants for K-SNR Asymptotic Relation across different Wireless Technologies

Wireless Technology	a	b
Zigbee	0.01	5.2983
Wi-Fi 802.11ac	44.916	0.4235
Wi-Fi 802.11ax	33.874	0.4151
Wi-Fi 802.11ad	45.391	0.4211

In addition, the presented parameters (as illustrated in table 3) may be used as a first aid in the building of a prototype to test the achieved throughput practically. In other words, the asymptotic relation (as in Equation 10) may be considered as a step forward to popularize the deployment of smart cities applications.

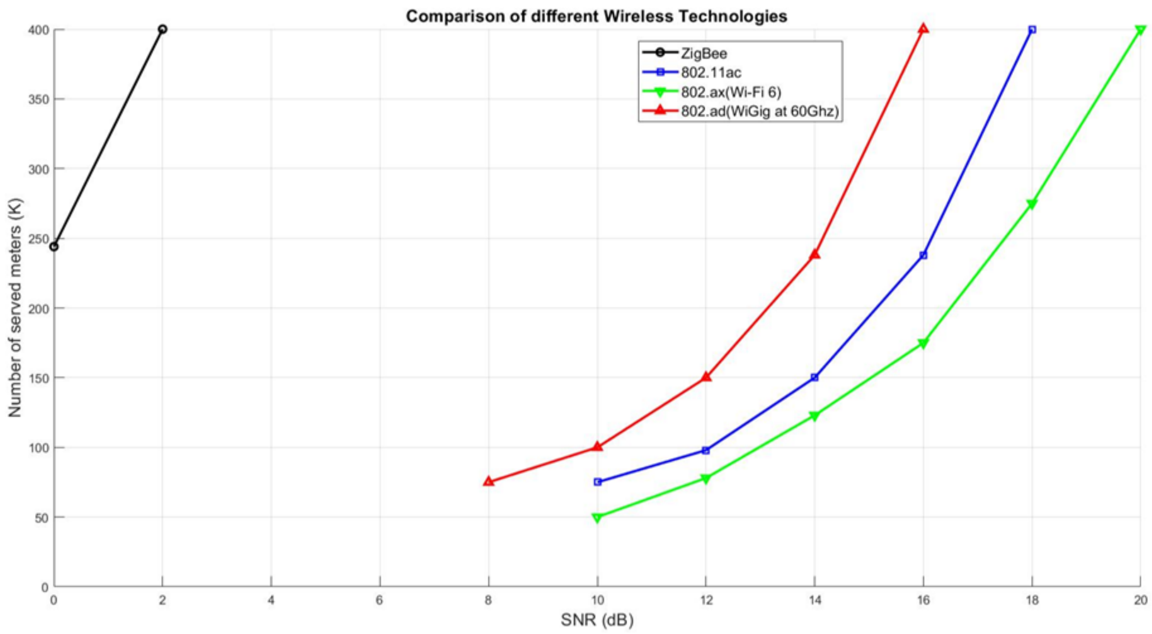

Figure 7. Number of served meters (K) vs. SNR levels for different wireless technologies.

5. CONCLUSION

This paper investigates the performance of a 60 GHz indoor smart metering system, by means of normalized EC (ε) as the primary performance metric. Monte Carlo simulations, incorporating Nakagami-m fading, close-in path loss model is used, as well as shadowing, and a Poisson point Process model for blockages distribution. To improve signal reception and enhance system reliability, the research proposes mitigation strategies such as deploying multiple receive antennas at the gateway and implementing diversity techniques, particularly maximum ratio combining (MRC).The main outcomes of this paper can be summarized as follows: Convergence of the normalized EC (ε) was observed after approximately 100 simulation trials, highlighting the importance of sufficient trials for accurate performance evaluation. Notably, the realistic random deployment model, both in the presence and absence of blockages, exhibited lower capacity compared to the idealized model, emphasizing the necessity of incorporating real-world scenarios in system design. Furthermore, the study revealed an inherent trade-off between connectivity and per-meter capacity. As the number of smart meters (K) increased, a corresponding decrease in normalized EC (ε) was observed across various SNR levels. This underscores the challenges posed by increased interference and limited bandwidth. Finally, a comparative analysis of various wireless technologies commonly employed in smart meter deployments was conducted. This analysis yielded an asymptotic relationship between the number of interfering smart meters (K) and SNR, providing valuable insights for deployment planning and optimization. Notably, 802.11ad (WiGig at 60 GHz) emerged as the superior technology, showing an 11.1% improvement over 802.11ac and a 20% improvement over 802.11ax. To build upon these findings, it is interesting to extend the analysis to include a larger user base with optimized power levels, the impact of mobility on system performance will be investigated, considering scenarios with mobile smart meters and dynamic blockage environments. Additionally, investigating the effect of different applications, where each smart meter is equipped with multiple sensors performing various functions could further enhance the system's versatility and reliability. The asymptotic obtained relation may be considered as a step forward to popularize the deployment of smart cities applications. These extensions would offer valuable insights into future work for optimizing smart metering systems in diverse and dynamic environments.

REFERENCES

[1] Gohar, Ali, and Gianfranco Nencioni. "The role of 5G technologies in a smart city: The case for intelligent transportation system." Sustainability 13, no. 9 (2021): 5188.

[2] Guevara, Leonardo, and Fernando Auat Cheein. "The role of 5G technologies: Challenges in smart cities and intelligent transportation systems." Sustainability 12, no. 16 (2020): 6469.

[3] Cvar, Nina, Jure Trilar, Andrej Kos, Mojca Volk, and Emilija Stojmenova Duh. "The use of IoT technology in smart cities and smart villages: similarities, differences, and future prospects." Sensors 20, no. 14 (2020): 3897.

[4] González-Zamar, Mariana-Daniela, Emilio Abad-Segura, Esteban Vázquez-Cano, and Eloy López-Meneses. "IoT technology applications-based smart cities: Research analysis." Electronics 9, no. 8 (2020): 1246.

[5] COLAK, Ilhami, Ramazan BAYINDIR, and Seref SAGIROGLU. "The effects of the smart grid system on the national grids." In 2020 8th International Conference on Smart Grid (icSmartGrid), pp. 122-126. IEEE, 2020.

[6] Abrahamsen, Fredrik Ege, Yun Ai, and Michael Cheffena. "Communication technologies for smart grid: A comprehensive survey." Sensors 21, no. 23 (2021): 8087.

[7] Xu, Yulin, and Shilong Jia. "Research on Application of 5G to Smart City." In IOP Conference Series: Earth and Environmental Science, vol. 760, no. 1, p. 012014. IOP Publishing, 2021.

[8] Khuntia, Mitrabinda, Debabrata Singh, and Sipra Sahoo. "Impact of Internet of Things (IoT) on 5G." In Intelligent and Cloud Computing, pp. 125-136. Springer, Singapore, 2021.

[9] Tetteh, Bright, and Kehinde Awodele. "Power system protection evolutions from traditional to smart grid protection." In 2019 IEEE 7th International Conference on Smart Energy Grid Engineering (SEGE), pp. 12-16. IEEE, 2019.

[10] Seker, Cihat, Muhammet Tahir Güneser, and Turgut Ozturk. "A review of millimeter wave communication for 5G." In 2018 2nd International Symposium on Multidisciplinary Studies and Innovative Technologies (ISMSIT), pp. 1-5. Ieee, 2018.

[11] Maham, Behrouz, and Petar Popovski. "Capacity analysis of coordinated multipoint reception for mmWave uplink with blockages." IEEE Transactions on Vehicular Technology 69, no. 12 (2020): 16299-16303.

[12] Shi, Jianfeng, Cunhua Pan, Wence Zhang, and Ming Chen. "Performance analysis for user-centric dense networks with mmWave." IEEE Access 7 (2019): 14537-14548.

[13] Roche, Edward M., and L. Walker Townes. "Millimeter wave “5G” wireless networks to drive new research agenda." Journal of Information Technology Case and Application Research 19, no. 4 (2017): 190-198.

[14] Bai, Tianyang, and Robert W. Heath. "Coverage and rate analysis for millimeter-wave cellular networks." IEEE Transactions on Wireless Communications 14, no. 2 (2014): 1100-1114.

[15] Cheng, Ming, Jun-Bo Wang, Yongpeng Wu, Xiang-Gen Xia, Kai-Kit Wong, and Min Lin. "Coverage analysis for millimeter wave cellular networks with imperfect beam alignment." IEEE Transactions on Vehicular Technology 67, no. 9 (2018): 8302-8314.

[16] Bhattacharyya, Sabyasachi, and G. Aruna. "Outage Probability Analysis of SNR for a MM Wave Beamsteered MIMO-MRC System." In 2019 International Conference on Wireless Communications Signal Processing and Networking (WiSPNET), pp. 246-251. IEEE, 2019.

[17] Govenker, Ratnakant Dinraj, Atharva Yashodhan Phatak, Rahul Bajpai, and Naveen Gupta. "Outage analysis of mmwave integrated device-to-device communication system under nakagami fading channel." In 2020 National Conference on Communications (NCC), pp. 1-6. IEEE, 2020.

[18] Turgut, Esma, and M. Cenk Gursoy. "Uplink performance analysis in D2D-enabled mmwave cellular networks." In 2017 IEEE 86th Vehicular Technology Conference (VTC-Fall), pp. 1-5. IEEE, 2017.

[19] Onireti, Oluwakayode, Lei Zhang, Ali Imran, and Muhammad Ali Imran. "Outage probability in the uplink of multitier millimeter wave cellular networks." IEEE Systems Journal 14, no. 2 (2020): 2520-2531.

[20] Kim, Minsu, and Jemin Lee. "Outage probability of UAV communications in the presence of interference." In 2018 IEEE Global Communications Conference (GLOBECOM), pp. 1-6. IEEE, 2018.

[21] Tuan, Nguyen Trong, Dong-Seong Kim, and Jae-Min Lee. "On the performance of cooperative transmission schemes in industrial wireless sensor networks." IEEE Transactions on Industrial Informatics 14, no. 9 (2018): 4007-4018.

[22] Dilli, Ravilla. "Performance analysis of multi user massive MIMO hybrid beamforming systems at millimeter wave frequency bands." Wireless Networks 27, no. 3 (2021): 1925-1939.

[23] Zhang, Shangwei, and Jiajia Liu. "Ergodic capacity analysis on MIMO communications in internet of vehicles." Mobile Networks and Applications 26 (2021): 923-939.

[24] Zhang, Shangwei, and Jiajia Liu. "Ergodic capacity analysis on MIMO communications in internet of vehicles." Mobile Networks and Applications 26 (2021): 923-939.

[25] Omer, Daroon Shaho, Mohammed Abdullah Hussein, and Luqman Mahmood Mina. "Ergodic capacity for evaluation of mobile system performance." Journal of Engineering 26, no. 10 (2020): 135-148.

[26] Hassan, Ahmad Kamal, and Muhammad Moinuddin. "Beamforming using exact evaluation of leakage and ergodic capacity of MU-MIMO system." Sensors 21, no. 20 (2021): 6792.

[27] Salimian Rizi, Fereshteh, and Abolfazl Falahati. "Ergodic capacity and symbol error rate analysis of a wireless system with α-μ composite fading channel." Wireless Personal Communications (2022): 1-16.

[28] Venugopal, Kiran, Matthew C. Valenti, and Robert W. Heath. "Device-to-device millimeter wave communications: Interference, coverage, rate, and finite topologies." IEEE Transactions on Wireless Communications 15, no. 9 (2016): 6175-6188.

[29] Kusaladharma, Sachitha, Zhang Zhang, and Chintha Tellambura. "Interference and outage analysis of random D2D networks underlaying millimeter-wave cellular networks." IEEE Transactions on Communications 67, no. 1 (2018): 778-790.

[30] Chun, Young Jin, Simon L. Cotton, Harpreet S. Dhillon, Ali Ghrayeb, and Mazen O. Hasna. "A stochastic geometric analysis of device-to-device communications operating over generalized fading channels." IEEE Transactions on Wireless Communications 16, no. 7 (2017): 4151-4165.

[31] Fatnassi, Wael, and Zouheir Rezki. "Reliability enhancement of smart metering system using millimeter wave technology." IEEE Transactions on Communications 66, no. 10 (2018): 4877-4892.

[32] Alyosef, Ayham, Stamatia Rizou, Zaharias D. Zaharis, Pavlos I. Lazaridis, Ahmed M. Nor, Octavian Fratu, Simona Halunga, Traianos V. Yioultsis, and Nikolaos V. Kantartzis. "A Survey on the Effects of Human Blockage on the Performance of mm Wave Communication Systems." In 2022 IEEE International Black Sea Conference on Communications and Networking (BlackSeaCom), pp. 249-253. IEEE, 2022.

[33] Carneiro de Souza, L., de Souza Lopes, C.H., de Cassia Carlleti dos Santos, R., Cerqueira Sodré Junior, A. and Mendes, L.L., 2022. A study on propagation models for 60 GHz signals in indoor environments. Frontiers in Communications and Networks, 2, p.757842.

[34] Sharmin, S., Boby, S.M. and Mahmud Boby, S., 2020. Characterization of WLAN System for 60 GHz Residential Indoor Environment Based on Statistical Channel Modeling. International Journal of Wireless and Microwave Technologies (IJWMT), 10(2), pp.42-58.

[35] Mohebi, Salman, Mattia Lecci, Andrea Zanella, and Michele Zorzi. "The challenges of Scheduling and Resource Allocation in IEEE 802.11 ad/ay." In 2020 Mediterranean Communication and Computer Networking Conference (MedComNet), pp. 1-4. IEEE, 2020.

[36] Oladimeji, Tolulope T., Pradeep Kumar, and Mohamed K. Elmezughi."Path Loss Measurements and Model Analysis in an Indoor Corridor Environment at 28 GHz and 38 GHz." Sensors 22, no. 19 (2022): 7642.

[37] Al-Saman, Ahmed, Michael Cheffena, Olakunle Elijah, Yousef A. Al-Gumaei, Sharul Kamal Abdul Rahim, and Tawfik Al-Hadhrami. "Survey of millimeter-wave propagation measurements and models in indoor environments." Electronics 10, no. 14 (2021): 1653.

[38] Huang, Li-Fei. "The Nakagami and its related distributions." WSEAS Trans. Math 15, no. 44 (2016): 477-485.

[39] Department of Energy & Climate Change, Smart Metering Equipment Technical Specifications, ver. 2, draft (London: Department of Energy and Climate Change, 2013(.